

The N M R of High Temperature Superconductors  
without Anti-Ferromagnetic Spin Fluctuations

Jamil Tahir-Kheli

First Principles Research, Inc.

8391 Beverly Blvd., Suite # 171, Los Angeles, CA 90048

www.rstprinciples.com

Abstract

A microscopic theory for the NMR anomalies of the planar Cu and O sites in superconducting  $\text{La}_{1.85}\text{Sr}_{0.15}\text{CuO}_4$  is presented that quantitatively explains the observations without the need to invoke anti-ferromagnetic spin fluctuations on the planar Cu sites and its significant discrepancy with the observed incommensurate neutron spin fluctuations. The theory is derived from the recently published ab-initio band structure calculations that correct LDA computations tendency to overestimate the self-coulomb repulsion for the half-filled Cu  $d_{x^2-y^2}$  orbitals for these ionic systems. The new band structure leads to two bands at the Fermi level with holes in the Cu  $d_{z^2}$  and apical O  $p_z$  orbitals in addition to the standard Cu  $d_{x^2-y^2}$  and planar O  $p$  orbitals. This band structure is part of a new theory for the cuprates that explains a broad range of experiments and is based upon the formation of Cooper pairs comprised of a  $k$  electron from one band and a  $k'$  electron from another band (Interband Pairing Model).

## Introduction

All current explanations<sup>1;2</sup> of the dramatically different NMR behaviors of the Cu and O nuclei separated by only 2.0Å in the CuO planes of high temperature superconductors are based on the existence of anti-ferromagnetic (AF) spin fluctuations on the Cu sites. The NMR difference is attributed to the delicate cancellation on the O sites of these AF fluctuations. The success of such models is dependent upon the AF spin correlation having a large peak very close or at wavevector  $(\pi; \pi)$ . Neutron scattering experiments have detected a spin correlation peak at incommensurate wavevectors  $(\pi; \pi + \delta)$  and  $(\pi + \delta; \pi)$  with  $\delta \approx 0.2$ , spoiling the initial success of the models<sup>3</sup>.

The models can be corrected by adding in next-nearest neighbor hyperfine couplings of the Cu atoms to the O sites to cancel the incommensurate fluctuations<sup>4</sup>, but the required hyperfine couplings are chemically too large. Finally, these models suffer from the lack of a microscopic derivation of the wavevector, temperature, and doping dependence they require the spin fluctuation function (i.e., the spin susceptibility  $\chi(\mathbf{q}; kT)$ ) to satisfy in order to fit experiments. Thus, we regard expressions for  $\chi(\mathbf{q}; kT)$  as empirically devised to fit the NMR experimental data.

Recently, we proposed an Interband pairing model (IBP)<sup>5;6</sup> for superconductivity that can explain the different Cu and O NMR without invoking AF fluctuations and the functional form of the spin susceptibility. In IBP, the incommensurate spin fluctuation peaks observed by spin neutron scattering arise naturally from the microscopic computed three dimensional (3D) band structure (but not the 2D band structure we computed previously), yet they do not lead to the NMR problems of AF fluctuation models.

The IBP model is based on the idea that in the vicinity of special symmetry directions, Cooper pairs comprised of a  $k_1$  electron from one band and a  $k_2$  electron from a different band are formed (interband pairs) and couple to standard BCS-like Cooper pairs ( $k_1$  and  $k_2$  from the same band) elsewhere in the Brillouin zone. In particular for LaSrCuO, the crossing occurs between a Cu  $d_{x^2-y^2}$  band and a Cu  $d_{z^2}$  band along the diagonals  $k_x = k_y$ .

Such a theory requires the existence of two bands at the Fermi level that can cross with optimal doping associated with the bands crossing at the Fermi level. Local Density Approximation (LDA) band structure computations done over a decade ago<sup>7</sup> and accepted implicitly by the physics community<sup>8</sup> as the correct starting point for developing theories of the cuprates find only a single Cu  $d_{x^2-y^2}$  and O p antibonding band at the Fermi level with all other bands well above or below the Fermi energy. As we argued previously,<sup>6</sup> such calculations are plagued by improperly subtracting only  $(1/2)J$  for a half-filled band from the  $d_{x^2-y^2}$  orbital energy rather than subtracting a full  $J$  due to the strong correlation in such ionic systems, where  $J$  is the  $d_{x^2-y^2}$  self-Coulomb repulsion. LDA calculations therefore, artificially raise the  $d_{x^2-y^2}$  and p antibonding band above the other Cu d bands. When we correct the orbital energy evaluation,<sup>6</sup> we find that in addition to the Cu  $d_{x^2-y^2}$  and O p orbitals, holes are created in the Cu  $d_{z^2}$  and apical O  $p_z$  orbitals leading to two bands at the Fermi level.

The IBP model has had great success explaining a broad spectrum of diverse high  $T_c$  experimental observations. These include the Hall effect, d-wave Josephson tunneling with coupling due to phonons, the doping sensitivity of the cuprates, resistivity, and the NMR (within the context of a 2D band structure with an approximate 3D structure added on).<sup>5</sup> Most recently, we have shown<sup>9</sup> that our band crossing at the Fermi level for optimal doping prevents the electron gas from adequately screening the attractive electron-phonon coupling as occurs in BCS superconductors, leading to a simple explanation for the observed  $T_c$  values in excess of standard BCS limits. In addition, the incommensurate neutron spin scattering and the anomalous mid-infrared absorption peak arise in a straightforward manner from our 3D bands.<sup>10</sup> Finally, the angle resolved photo-emission spectroscopy (ARPES) and in particular, the observed so called pseudo-gap (a gap on the Fermi surface in the normal state) for underdoped cuprates and its disappearance for overdoping have been explained as due to the rapid change in the orbital characters of the two bands near the energy of the band crossing and the fact that k states with primarily  $d_{z^2}$  character do not have resolvable quasiparticle peaks in the ARPES spectra.<sup>11</sup> This leads to the incorrect assignment of the Fermi surface in underdoped systems as the crossover

surface between dominant  $d_{x^2-y^2}$  and  $d_{z^2}$  characters and hence the erroneous conclusion that a pseudo-gap has opened above  $T_c$  on the Fermi surface. The reason for the lack of a sharp quasiparticle peak in the ARPES spectra for  $d_{z^2}$  electrons is because there is no great anisotropy in its dispersion in the CuO planes versus its dispersion normal to the planes. This is in contrast to the almost 2D dispersion of  $d_{x^2-y^2}$  and leads to a large linewidth of  $d_{z^2}$  from the intermediate excited photo-electron state that is added to the physically interesting linewidth of the initial electron state.

In this paper, we derive the key NMR observations based upon the detailed 3D band structure we obtained recently.<sup>12</sup> This explanation supersedes the NMR discussion in our previous work that was based upon a 2D band with an approximate 3D dispersion and is significantly different in the details. The essential features remain the same. These are:

- 1.) the interesting region of the Brillouin zone (BZ) for the upper band is the vicinity of the saddle point density of states (DOS) at  $(\pi/a; 0)$  or  $(\pi/a; 0; \pi/c)$  for the 3D zone and the relevant region for the lower band is near  $(\pi/a; \pi/a)$  that is at the top of this band. Both the saddle point and the top of the lower band at  $(\pi/a; \pi/a)$  are close to the Fermi energy (less than or on the order of  $0.08$  eV).
- 2.) the character of the lower band  $k$  states near  $(\pi/a; \pi/a)$  has reduced  $O_p$  and  $2s$  character. The reduced  $O_p$  is due to the  $O$  sites forming a bonding combination in order to couple to  $d_{z^2}$  at  $(\pi/a; \pi/a)$ .  $O_{2s}$  is reduced because it cannot couple to  $d_{z^2}$  and  $d_{x^2-y^2}$  by symmetry.
- 3.) the Cu spin relaxation anisotropy of  $3:4$  for magnetic fields in the plane versus perpendicular to the CuO planes is due to the small amount of Cu  $d_{xy}$  and its spin orbital coupling to  $d_{x^2-y^2}$ .

A new piece of chemistry appears in this paper in order to produce the small increase ( $0.1\%$ ) in the  $O$  spin relaxation rate over temperature ( $1/T_1T$ ) from  $50K$  to  $300K$  that was not required in the 2D model. That is the Jahn-Teller alternating tilt of the  $CuO_6$  octahedra reducing the crystal point group from  $D_{4h}$  to  $D_{2h}$  and changing the Bravais lattice from body-centered tetragonal to one-face-centered orthorhombic.<sup>7</sup> The distortion

splits the saddle point peak in the DOS at wavevector  $(\pi/a; 0; \pi/c)$  and  $(0; \pi/a; \pi/c)$  into two peaks. Hund-Rothery and Jahn-Teller type arguments suggest the material will self-adjust to place its Fermi level between these two peaks because the unperturbed saddle point singularity is so close to the Fermi energy. We argue, but do not compute, that the distortion leads to the  $\rho_1 = T_1 T$  increase with  $T$  and suggest this is the reason these systems have a tendency to self-dope to optimal doping for the highest  $T_c$ .

### 3D Band Structure

The 3D Fermi surface for optimally doped  $\text{La}_{1.85}\text{Sr}_{0.15}\text{CuO}_4$  is shown in figures 1(a-d) at various fixed  $k_z$  values.<sup>12</sup> The range of values of  $k_z$  is  $-\pi/c < k_z < \pi/c$  and  $k_x, k_y$  vary between  $-\pi/a$  and  $\pi/a$  where  $a = 3.8\text{\AA}$  and  $c = 13.2\text{\AA}$  are the doubled rectangular unit cell parameters. As  $k_z$  is increased from 0 to  $\pi/18 = \pi/c$ , the Fermi surface is very similar to the standard LDA one band result with a hole-like surface centered around  $(\pi/a; \pi/a)$ . At  $k_z = \pi/18 = \pi/c$ , the top of the lower band is reached and as  $k_z$  is increased further, a second hole-like Fermi surface appears centered around  $(0; 0)$ . This arises from the 3D coupling of the apical  $\text{O } p_z$  orbitals in one layer to its neighboring apical  $\text{O } p_z$  in another layer. At  $k_z = \pi/54 = \pi/c$ , the two Fermi surfaces touch along the diagonal that is the only symmetry allowed crossing. Further increasing of  $k_z$  to its upper limit of  $\pi/c$  splits the two surfaces into three with a hole-like surface centered around the diagonal and two electron-like surfaces centered at  $(\pi/a; 0)$  and  $(0; \pi/a)$ .

Figures 2(a-d) show the total density of state (DOS) and the bare DOS for  $\text{Cu } d_{z^2}$ ,  $d_{x^2-y^2}$  and  $\text{O } p$ . Note the large DOS peak just below the Fermi level due to the almost pure 2D character of the bands at  $(\pi/a; \pi/a)$ . At  $(\pi/a; \pi/a)$ , the lower band is composed of  $d_{z^2}$  and the bonding combination of  $p$ . This is the most unstable  $d_{z^2}$  state at this  $k$  vector. There is no  $d_{x^2-y^2}$  or  $\text{O } 2s$  due to symmetry. Because the  $p$  orbitals are in a stabilizing bonding combination, the most unstable  $d_{z^2}$  state will not have much  $p$  character at all. Thus, the  $k$  states that contribute to the peak in the DOS just below the Fermi level in the vicinity of  $(\pi/a; \pi/a)$  have very little  $d_{x^2-y^2}$ ,  $p$ , and  $\text{O } 2s$  characters.

The bare DOS for a given band is defined as the product of the average orbital

character for the band at a given energy times the DOS of the band. The total bare DOS for each orbital is the sum of the bare DOS from each band and is the relevant quantity for the NMR. Physically, the total bare DOS of an orbital is the number of electrons in the orbital per unit of energy.

The most important thing to notice from these figures is the difference in the behaviors of the Cu  $d_{z^2}$  bare DOS versus  $d_{x^2-y^2}$  and O p.  $d_{z^2}$  is very sensitive to the large DOS that arises from the lower band near ( $\approx a$ ;  $\approx a$ ) whereas, both the total bare DOS for  $d_{x^2-y^2}$  and p are not. This is the fundamental reason for the difference in the Cu and O spin relaxation rates.

Figures 3(a-c) show the orbital character for each band. One can see that the two bands trade off their orbital characters when the bands cross.

## The Cu and O NMR

We use standard expressions for the nuclear spin relaxation rates due to delocalized electrons that are well described by simple Bloch states to form bands.<sup>13;14</sup> All of the relevant expressions for computing the spin relaxation rates on the planar Cu and O sites due to  $d_{x^2-y^2}$ ,  $d_{z^2}$  and p are explicitly written down in reference 5. We do not reproduce them all here. Instead, we will write down the general form of the expression (equation (61) in the above reference) to clarify our discussion of the results.

The general expression for the spin relaxation rate in the cuprates where we neglect the contribution from the Cu 4s and O 2s contact terms and the core polarization is,

$$\frac{1}{T_1} = 2 \frac{2}{h} \left( \frac{e}{h} \hbar \right)^2 \int d f(\epsilon) (1 - f(\epsilon)) \frac{1}{r^3} [W_{dip}(\epsilon) + W_{orb}(\epsilon)]; \quad (1)$$

where  $f(\epsilon)$  is the Fermi-Dirac function,  $f(\epsilon) = 1/(e^{(\epsilon - \mu)/k_B T} + 1)$  at energy  $\epsilon$  and  $\mu$  is the chemical potential.  $\gamma_e$  and  $\gamma_n$  are the electronic and nuclear gyromagnetic ratios,  $\langle 1/r^3 \rangle$  is the mean value of  $1/r^3$  for the relevant orbital,  $W_{dip}(\epsilon)$  is a function of the bare density of states of the orbitals for dipolar relaxation, and  $W_{orb}(\epsilon)$  is the similar expression for orbital relaxation.

For Cu relaxation with the magnetic field normal to the CuO planes (z-axis),  $W_{\text{dip}}$  and  $W_{\text{orb}}$  are given by,

$$W_{\text{dip}}^z(\epsilon) = \frac{1}{72} [6N_{d_{x^2-y^2}}(\epsilon)N_{d_{z^2}}(\epsilon) + N_{d_{x^2-y^2}}(\epsilon)N_{d_{x^2-y^2}}(\epsilon) + N_{d_{z^2}}(\epsilon)N_{d_{z^2}}(\epsilon)]; \quad (2)$$

$$W_{\text{orb}}^z(\epsilon) = 0; \quad (3)$$

where  $N_{(d_{x^2-y^2})}(\epsilon)$  and  $N_{(d_{z^2})}(\epsilon)$  are the total bare density of states for their respective orbitals. We take  $\langle 1/r^3 \rangle = 6.3 \text{ a.u.}$  for  $\text{Cu}^{15}$  and make the crude approximation<sup>5</sup> of  $3.0 \text{ a.u.}$  for O.

The inclusion of Cu 4s and the effects of core polarization will lead to a small change in the computed magnitude of the Cu spin relaxation and Knight shift, but should not change the overall qualitative behavior. The O 2s can increase the magnitude of the O relaxation rate by an order of magnitude due to its large density at the O nucleus but as discussed above, cannot alter the qualitative behavior of the relaxation and Knight shift curve because by symmetry, no 2s character appears at  $(\epsilon = a; \epsilon = a)$ .

In most metals, the bare densities of states that appear in equations (2) and (3) can be taken to be constant over the range  $\sim kT$  around the Fermi level. The integral in equation (1) is thereby over  $f(1-f)$  and is equal to the temperature  $kT$ . Hence,  $1/T_1T$  is a constant. Due to the band crossing, the closeness of the Fermi level to the saddle point singularity in the DOS at  $(\epsilon = a; \epsilon = c)$  and the top of the lower band, the bare densities of states cannot be taken to be constant over the range of energies relevant for computing the NMR. In addition, the chemical potential increases with increasing temperature in order to maintain particle conservation. Thus,  $\mu$  must be solved for self-consistently at every temperature.

Figures 4a and 4b show the calculated Cu and O spin relaxation rates over temperature  $1/T_1T$  for a z-axis magnetic field. The Cu  $1/T_1T$  initially rises due to the sharp increase in the  $d_{z^2}$  bare DOS just below the Fermi level from the DOS peak at  $(\epsilon = a; \epsilon = a)$ . As the temperature is further increased, the chemical potential increases to maintain particle conservation and the integral in equation (1) "falls over" the top of the lower band

leading to the sharp decrease in the relaxation. The values we obtained are approximately a factor of 2 larger than experiment but the most important point is the percentage increase from 50K to the maximum and the approximately factor of 1.4 decrease from the maximum value to the value at 300K are compatible with experiment where the increase is 10-30% and the decrease is about factor of 2.<sup>3</sup>

In contrast, the  $\rho^{-1} = T_1 T$  decreases by 8% as the temperature is increased. This is due to the lack of the  $(\sigma_a; \sigma_a)$  peak in the bare DOS for p and the decrease in its bare DOS as the energy is increased above the  $T = 0$  Fermi level. The relaxation is more sensitive to bare DOS values above the  $T = 0$  Fermi level due to the increase in  $\rho$ . These numbers are about a factor of 5 smaller than experimental values. Inclusion of O 2s character can easily produce an increase of a factor of 5-10 without changing the qualitative behavior.

The most important point to note here is that the decrease of the O relaxation is very small compared to the scale of the Cu relaxation decrease. Although, with the present calculations the small observed increase is not reproduced, we have already attained considerable success in obtaining such a dramatic difference in the Cu and O NMR. By considering the orthorhombic  $\text{CuO}_6$  tilt in the following section, we will argue that in fact, the observed increase can be obtained by our model.

The expressions for the various Knight Shifts are explicitly written down in reference 5 and are not reproduced here. As before<sup>5</sup>, we must assume that  $d_{z^2}$  and Cu 4s interfere such that the net dipolar field due to the  $d_{z^2}$  and the Cu 4s hybrid is of the opposite sign of a single  $d_{z^2}$  in order to lead to an increase in the Cu Knight shift with increasing temperature and the lack of strong temperature dependence of the shift for a z-axis field. This is discussed in detail in reference 5.

The one additional point in favor of the sign flip of the dipolar field of  $d_{z^2}$  due to interference with the 4s for our 3D model as compared to our 2D model is that in the 3D model,  $d_{z^2}$  holes appear in the vicinity of  $(0;0; \pi/c)$ . At  $(0;0)$ , 4s character will mix with  $d_{z^2}$  and by symmetry p cannot couple to them. Thus, one expects the 4s to mix into the  $d_{z^2}$  to increase the size of the d orbital in the planar directions, or in other words, interfere

with  $d_{z^2}$  with the correct sign to lead to a net sign flip of the dipolar field.

Figures 5a and 5b show the Cu and O z-axis Knight shifts. The O Knight shift does not include O 2s and decreases with increasing temperature. The Cu shift increases with increasing temperature and hence does not track the spin relaxation curve in agreement with experiment. This is due to the fact that for relaxation, the DOS appear twice (squared) in the relaxation expression because the initial and final state probabilities of the relaxing electron must be multiplied together. For the Knight shift, only a single power of the DOS appears. The Cu relaxation is therefore more sensitive than the shift to the sharp increase in the DOS due to  $(\uparrow a; \uparrow a)$  just below the Fermi level.

Note also the contribution to the temperature dependence of the Cu shift from  $d_{x^2 - y^2}$  is much smaller than the contribution from  $d_{z^2}$ . In figure 5a, we plot the  $d_{x^2 - y^2}$  contribution multiplied by 10 and minus the  $d_{z^2}$  shift to incorporate the sign flip interference from Cu 4s. The scale of the Cu shift is consistent with with experiments.

#### Orthorhombic Distortion

The orthorhombic  $\text{CuO}_6$  octahedra tilt in  $\text{La}_{1.85}\text{Sr}_{0.15}\text{CuO}_4$  splits the DOS peak at  $(\uparrow a; 0; \uparrow c)$  and  $(0; \uparrow a; \uparrow c)$  into two peaks at energy shifts  $\pm \epsilon_0$  where  $\epsilon_0$  is the original energy. This leads to a local gap in the energy between these two values in the vicinity of the saddle point. As the contribution to the DOS is large here, one expects the total DOS to be much smaller between the two peaks. Chemically, one expects the size of  $\epsilon_0$  to be on the order of 0.01 - 0.05 eV or greater. The Fermi level will therefore fall between the two peaks. The overall effect on the Cu NMR will be small due to the dominance of the  $(\uparrow a; \uparrow a)$  peak for Cu. On the other hand, this distortion will dramatically change the O NMR from slightly decreasing to slightly increasing as observed by experiment. We believe this is the reason for the O NMR increase with temperature for  $\text{LaSrCuO}$ .

One also expects the system will adjust itself to place its Fermi level between the two peaks in order to lower its total free energy. This is essentially a Hund-Rothery or Jahn-Teller type argument. Such a mechanism provides a simple explanation for the tendency of several cuprates to "self-dope" to the optimal doping for  $T_c$ .

## Conclusions

We have presented a theory for the NMR of LaSrCuO that explains the observed different Cu and O relaxations as arising from two bands with Cu  $d_{x^2-y^2}$ ,  $d_{z^2}$ , planar O  $p_x$ , and apical O  $p_z$  characters. These bands were derived *ab initio*<sup>6;12</sup> by correcting the improper accounting of the self-coulomb contribution to the orbital energy in LDA band structure calculations. The theory resolves the NMR anomalies with a microscopic picture that does not require the introduction of anti-ferromagnetic spin fluctuations and it's corresponding disagreement with the observed incommensurate neutron spin fluctuations.

The splitting of the saddle point singularity in the density of states at  $k$  vector  $(\pi/a; 0; \pi/c)$  and  $(0; \pi/a; \pi/c)$  by the CuO<sub>6</sub> orthorhombic distortion changes the O NMR from monotonically decreasing with increasing temperature to monotonically increasing with temperature by splitting the peak into two peaks.

## Acknowledgments

We wish to thank Jason K. Perry with whom all parts of this work was discussed. We also wish to thank William A. Goddard III for his insight and encouragement during the development of the ideas presented here and in previous publications.

## REFERENCES

1. F. Mila and T. M. Rice, *Physica C* 157, 561 (1989)
2. D. Pines, *Physica C* 282, 273 (1997)
3. R. E. Walstedt, B. S. Shastry, and S-W. Cheong, *Phys. Rev. Lett.* 72, 3610 (1994)
4. Y. Zha, V. Barzkin, and D. Pines, *Phys. Rev. B* 54, 7561 (1996)
5. J. Tahir-Kheli, *Phys. Rev. B* 58, 12307 (1998)
6. J. K. Perry and J. Tahir-Kheli, *Phys. Rev. B* 58, 12323 (1998); J. K. Perry, *J. Phys. Chem.* (submitted), [xxx.lanl.gov/abs/cond-mat/9903088](http://xxx.lanl.gov/abs/cond-mat/9903088), [www.rstprinciples.com](http://www.rstprinciples.com)
7. W. E. Pickett, *Rev. Mod. Phys.* 61, 433 (1989) and references therein
8. P. W. Anderson, *The Theory of Superconductivity in the High-T<sub>c</sub> Cuprates* (Princeton, 1997), p. 33

9. J. Tahir-Kheli, Phys. Rev. Lett. (submitted), [www.rstprinciples.com](http://www.rstprinciples.com)
10. J. Tahir-Kheli, (to be published)
11. J.K. Perry and J. Tahir-Kheli, Phys. Rev. Lett. (submitted), [xxx.lanl.gov/abs/cond-mat/9908308](http://xxx.lanl.gov/abs/cond-mat/9908308), [www.rstprinciples.com](http://www.rstprinciples.com)
12. J.K. Perry and J. Tahir-Kheli, Phys. Rev. Lett. (submitted), [xxx.lanl.gov/abs/cond-mat/9907332](http://xxx.lanl.gov/abs/cond-mat/9907332), [www.rstprinciples.com](http://www.rstprinciples.com)
13. C.P. Slichter, Principles of Magnetic Resonance Third Edition (Springer-Verlag, 1990)
14. A. Abragam, Principles of Nuclear Magnetism (Oxford, 1961)
15. A. Abragam and B. Bleaney, Electron Paramagnetic Resonance of Transition Ions (Dover, 1986), p. 458

## Figure Captions

- 1 (a-d). The Fermi surface for a.)  $k_z = 0$ , b.)  $k_z = 1.30 \text{ \AA}^{-1}$ , c.)  $k_z = 1.54 \text{ \AA}^{-1}$ , and d.)  $k_z = 2 \text{ \AA}^{-1}$ .
- 2 (a-d). The density of states of the two bands and the bare density of states for Cu  $d_{x^2-y^2}$ ,  $d_{z^2}$ , and O p in units  $1/(\text{eV spin unit cell})$ .
- 3 (a-c). The orbital characters for the Cu  $d_{x^2-y^2}$ ,  $d_{z^2}$ , and O p orbitals.
- 4 (a,b). The Cu and O spin relaxation rate over temperature for a z-axis magnetic field. The O curve is only computed for the p orbital. Including O 2s will not change the qualitative behavior of the curve, but will increase its magnitude.
- 5 (a,b). The Cu and O Knight shifts. The contribution from  $d_{x^2-y^2}$  is multiplied by a factor of 10 and minus the  $d_{z^2}$  shift is plotted due to the argued sign arising from interference with Cu 4s. The O shift only includes the contribution arising from p.

Figure 1

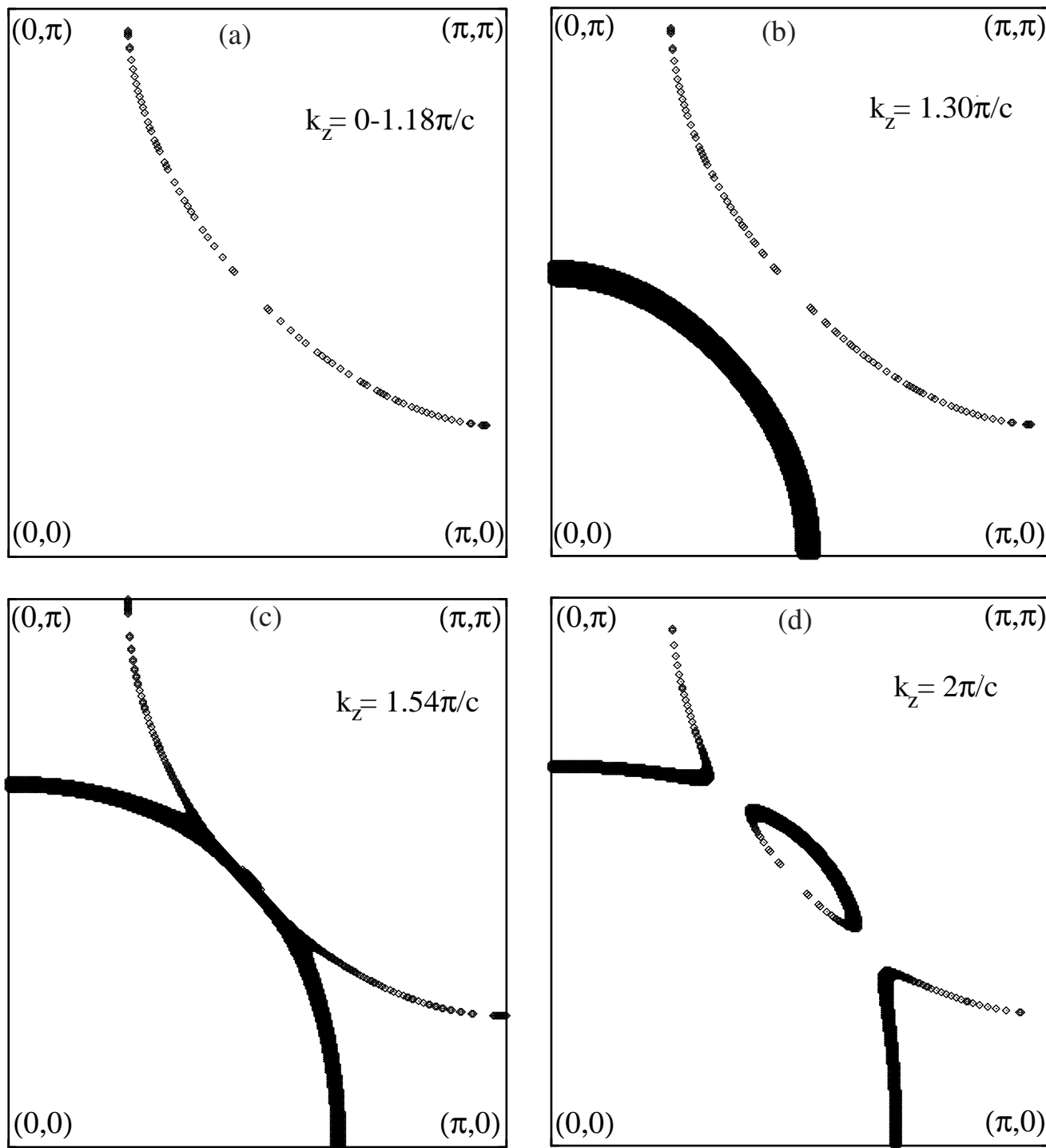
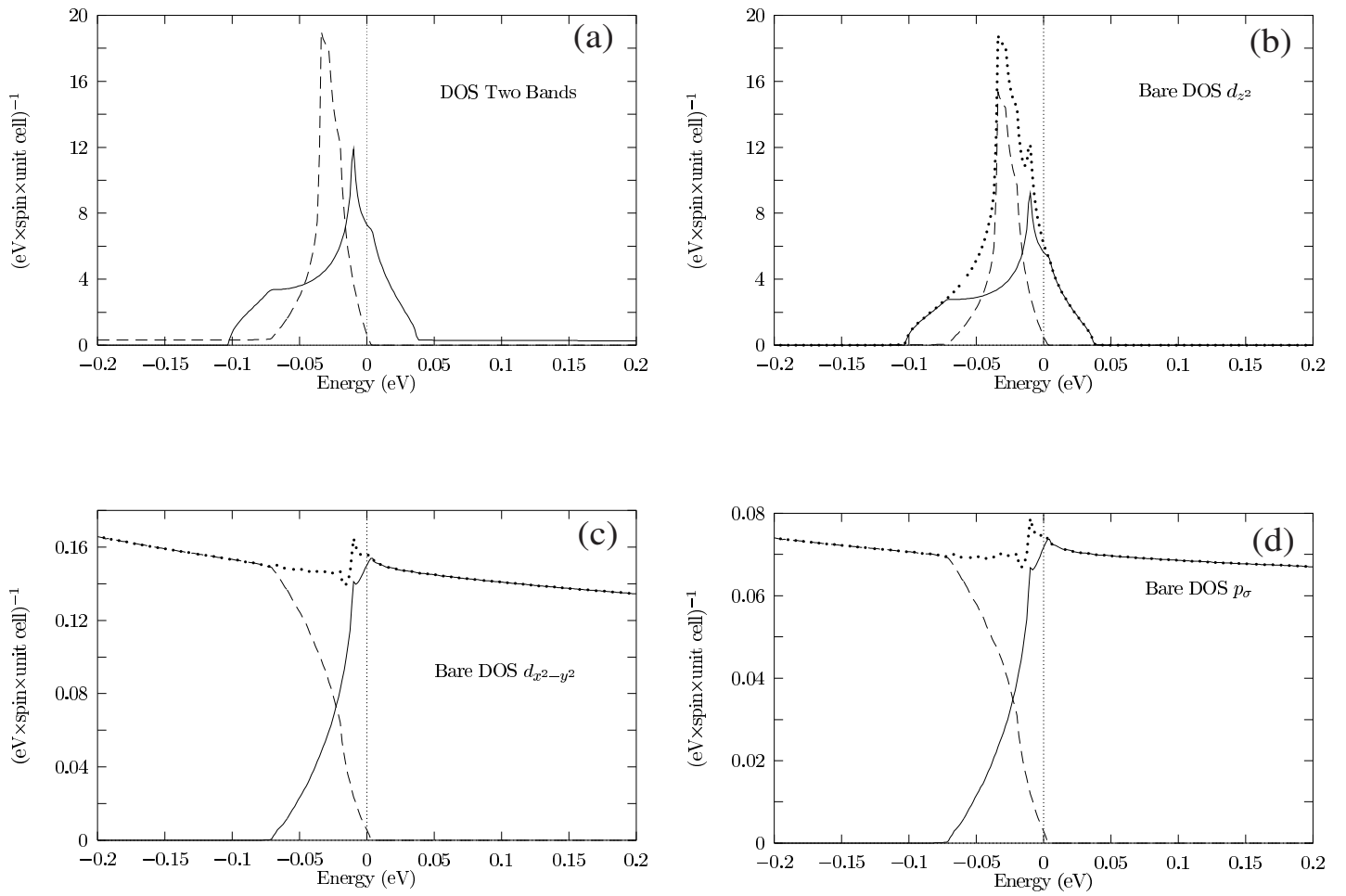


Figure 2



### Figure 3

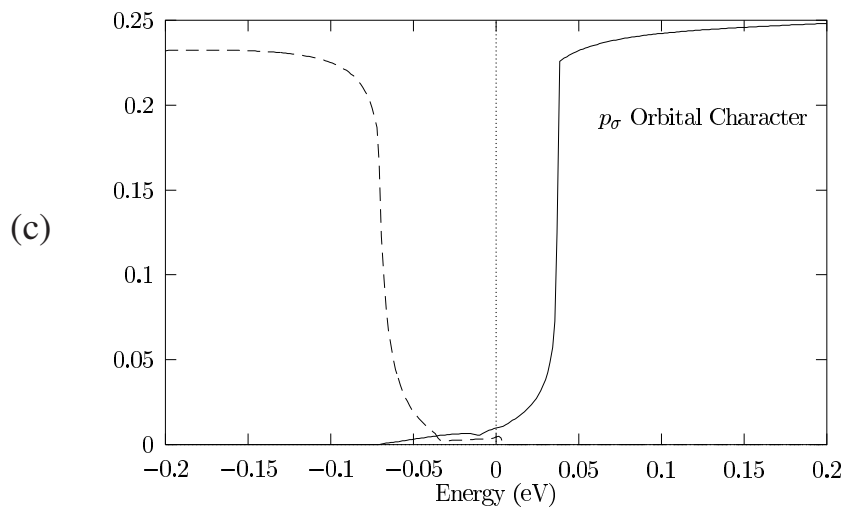
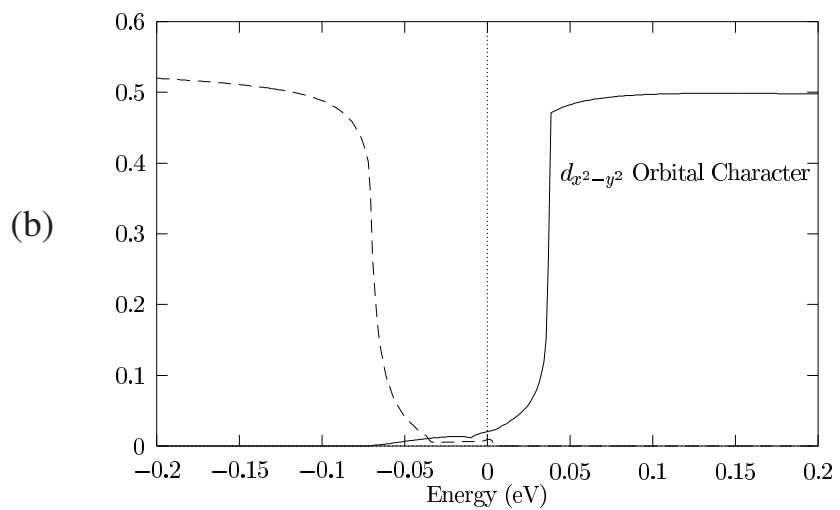
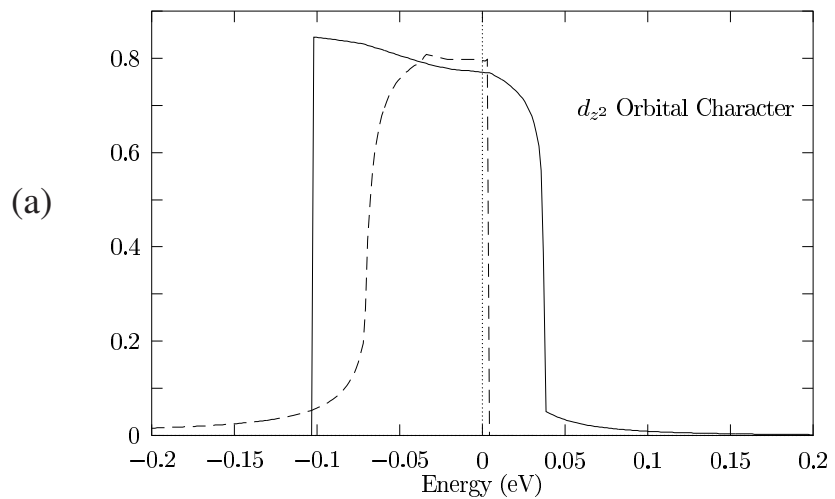


Figure 4

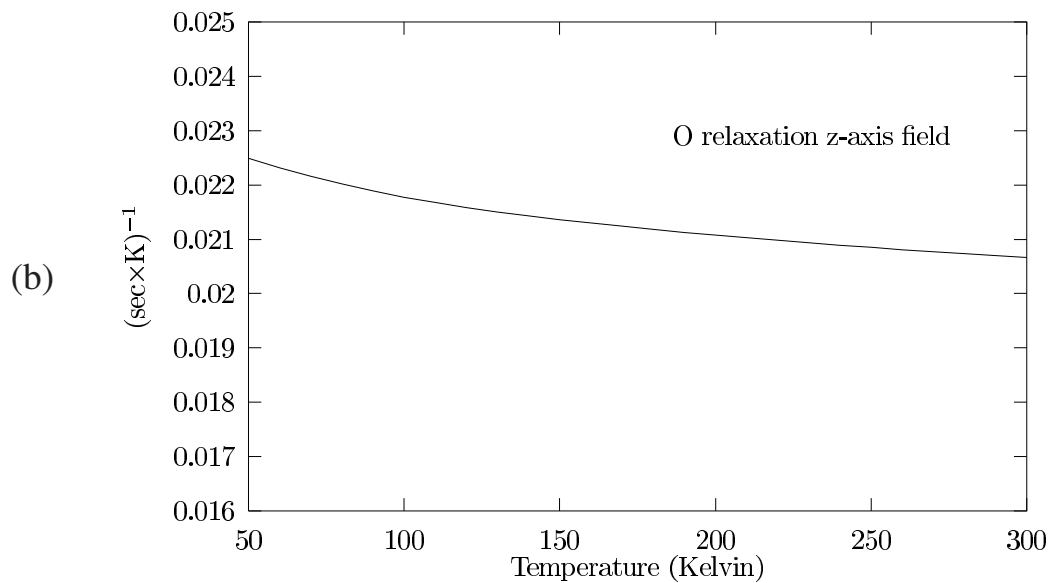
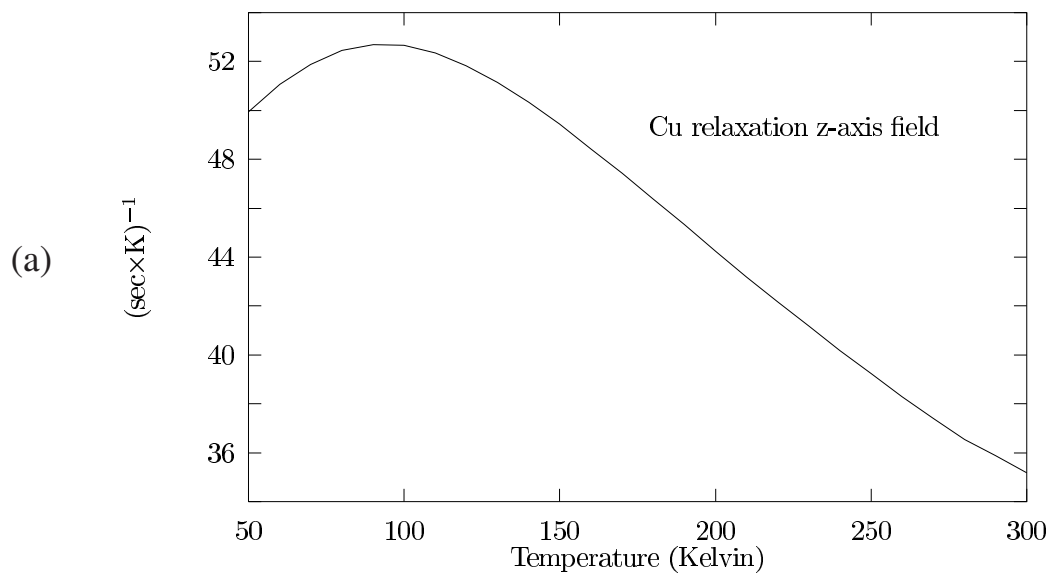


Figure 5

